Original papers

Med Ultrason 2024, Vol. 26, no. 2, 160-167
DOI: 10.11152/mu-4335

Comparison between combined ultrasounds and magnetic resonance imaging in the differentiation of benign and malignant breast lesions: a cross-sectional study

Chaoxi Li, Dehui Wen, Haiyong Lu

Department of Ultrasound Medicine, The First Affiliated Hospital of Hebei North University, Zhangjiakou, China

Abstract

Aim: To explore the performance of single or combined ultrasound (US) in diagnosing malignant breast lesions, and then compare the results with a magnetic resonance imaging (MRI) aspect. **Material and methods:** Patients' demographics, tumor markers, and imaging examination were collected. Diagnostic models based on B-mode, color Doppler ultrasounds (CDU), strain elastography (SE), MRI, B-mode US + CDU, B-mode US + SE, and B-mode US + CDU + SE were developed using logistic regression analysis. The performance was assessed using the area under the curve (AUC) with 95% confidence intervals (CIs). Performance of MRI and B-mode US + CDU was compared using DeLong analysis. **Results:** For single imaging modality, MRI showed the best performance, with AUC of 0.938 (95%CI: 0.888-0.988). For combined US modalities, combination of B-mode US and CDU had the best performance, with AUC of 0.948 (95%CI: 0.877-1.000). There was no significant difference in the diagnostic performance between the combination of B-mode US and CDU and MRI ($p>0.05$). **Conclusions:** Our study found the performance of B-mode + CDU was comparable to MRI. Our findings suggested that the combination of B-mode US and CDU was recommended to diagnose malignant breast lesions in order to save time and expense and provide guidance to make decisions for a biopsy.

Keywords: ultrasound; color Doppler; magnetic resonance imaging; breast lesions

Introduction

Breast cancer is the most frequently diagnosed cancer in women and has been the second leading cause for cancer-related death [1]. Since the mid-2000s, the incidence of breast cancer continues to increase slowly by about 0.5% per year in female [2]. The mortality of female breast cancer peaked in 1989 and has declined by 42% since then [3]. For the combination of all stages, a 5-year relative survival rate of patients with breast cancer is nearly 90% after diagnosis [3]. The World Health Organization (WHO) attributes this to the early identification and improved diagnostic methods [4].

Magnetic resonance imaging (MRI) is an advanced diagnostic modality, which is currently used for a supplementary diagnosis of breast cancer in a high-risk population, with excellent sensitivity and specificity [5]. However, this modality is relatively expensive and time-consuming [6]. Efforts to decrease the use of expensive imaging examinations while preserving diagnostic accuracy are necessary. In this context, ultrasound (US) is an ideal alternative because it provides both morphologic and functional information about breast tumors at a low cost [7]. Apart from morphologic imaging with standard B-mode, functional strain elastography (SE) and color Doppler ultrasounds (CDU) have been reported [8]. CDU helps to judge breast lesions according to the vascular distribution and hemodynamic information [9]. On SE, images are generated by displacement of tissues from manual compression or a low-frequency US pulse [10]. A study has shown that CDU and SE used in combination could improve the diagnostic value of B-mode US alone

Received 26.07.2023 Accepted 04.01.2023
Med Ultrason
2024, Vol. 26, No 2, 160-167
Corresponding author: Chaoxi Li
Department of Ultrasound Medicine, The First Affiliated Hospital of Hebei North University, 12 Changqing Road, Qiaoxi District, Zhangjiakou 075000, Hebei Province, China
Phone: +86 13831381011
E-mail: lichaoxi_umd@hotmail.com

in distinguishing malignant from benign breast lesions [9]. However, whether the diagnostic value of US modalities used alone or in combination could be an alternative for MRI needs to be further explored.

Therefore, the aim of this study was to assess the diagnostic value of B-mode US, CDU, and SE alone or in combination in distinguishing malignant from benign breast lesions, and then to compare it with that of MRI.

Material and methods

Study design and population

This was a cross-sectional study, which was performed in the First Affiliated Hospital of Hebei North University from April 2020 to October 2021.

Inclusion criteria: age ≥18 years old; with newly diagnosed one or more breast lesions; classifying as Breast Imaging Reporting and Data System (BI-RADS) category 4 or 5 on B-mode US; scheduling for a core needle biopsy and/or surgical excision; agreeing to participate in this study; and signing the informed consent form.

Exclusion criteria: Women in pregnancy or lactation; receiving microwave ablation, radiofrequency ablation, radiotherapy, chemotherapy, and biopsy before examination; or who had other concurrent malignant tumors.

If the patient had more than one lesion, the largest or the most suspicious one was selected as a target lesion for this study.

Ethical approval for this study was obtained from the local ethics committee (approval NO. W2020025) and written informed consent was obtained prior inclusion.

Data collection

Data were collected based on demographics (age, height, weight, family history, and comorbidities), tumor markers [carcinoembryonic antigen (CEA) and carbohydrate antigen 15-3 (CA15-3)], and imaging examination. Body mass index (BMI) was calculated by dividing weight (kg) by height^2 (m^2) [11]. Data on imaging examination were collected based on B-mode US [BI-RADS category, lesion location, tumor maximum diameter, and longitudinal/transverse diameter (L/T)], CDU [pulsatility index (PI), and resistance index (RI)], SE (elasticity score) and MRI [apparent diffusion coefficient (ADC)].

US examination and MRI

B-mode US

Patients were placed in the supine position and raised arms to fully expose breasts and armpits for B-mode US. Breast tissues were scanned from left to right and from outside up to inside down, and lymph nodes in armpits and clavicle were also scanned. The characteristics of breast tissue morphology, structure and echo were observed. The location, morphology, size, longitudinal/transverse diameter (L/T), boundary, and internal echo of the lesions were recorded after finding the lesions, which were then classified using BI-RADS. Lesions of BI-RADS category 4 and above were selected for CDU and SE. After lesions were clearly displayed on B-mode US, they were successively switched to CDU and SE.

CDU

For CDU (MyLab Twice End, Esaote, Italy), The frequency of high-frequency probe was set at 7-12 MHz, and hemodynamic characteristics of lesion sites were observed. The PI and RI of each lesion were calculated using computer integrated software. During this calculation, the inspector selected the best cycle from the Doppler waveform and manually placed the cursor at the maximum systolic and minimum diastolic velocities.

SE

The region of interest (ROI) was selected, and the size of ROI was adjusted to about twice that of the lesion. The lesion was placed in the center of the ROI. The probe was perpendicular to the body surface and pressure slightly applied and vibration to ensure the pressure and pressure release frequency within the normal range. After stabilization, the image was stored, and elasticity score was used to differentiate benign lesions from breast cancer according to lesion hardness.

MRI

MRI examination (Ingenia3.0T, Philips, Netherlands) was performed using breast specific 8-channel phased-array coil. All patients were scanned for T1-weighted imaging (T1WI), T2-weighted imaging, and diffusion weighted imaging (DWI). The ROI was delineated from these three aspects, and ADC values were calculated. The average value of the three measurements was taken. When delineating ROI, it should include the solid part of tumors as much as possible, avoiding necrosis, cystic degeneration, fat, and bleeding regions.

Pathologic diagnosis

The final diagnosis (benign or malignant) was performed by histopathology after surgical excision or US-guided core needle biopsy. A breast pathologist with 15 years of experience blinded to results of US scans, made all the diagnoses.

Development of the model

The patients were divided into training set and testing set according to the ratio of 7: 3. The logistic regression model was developed based on the B-mode US (BI-RADS category, tumor maximum diameter), CDU (PI and RI), SE (elasticity score), MRI (ADC), B-mode US + CDU, B-mode US + SE, and B-mode US + CDU + SE. The model for MRI and B-mode US + CDU were further considered age, BMI, and CA15-3. Model performance was assessed by calculating the area under the curve

(AUC) with 95% confidence intervals (CIs), sensitivity, specificity, positive predictive value (PPV), negative predictive value (NPV), and accuracy.

Statistical analysis

Measurement data of normal distribution were described as mean ± standard deviation (mean ± SD) and differences between the two groups were compared using t-test. Measurement data of non-normal distribution were described as median and interquartile range [M (Q1, Q3)], and differences between two groups were compared using Mann-Whitney U rank-sum test. Counting data were described as number (n) and percentage (%), and the chi-squared test was used to compare intergroup differences. DeLong analysis was used to compare the performance of models based on MRI and B-mode US + CDU. All statistical analysis was performed using SAS 9.4 (SAS Institute Inc., Cary, NC, USA), and statistical significance was shown as $p<0.05$.

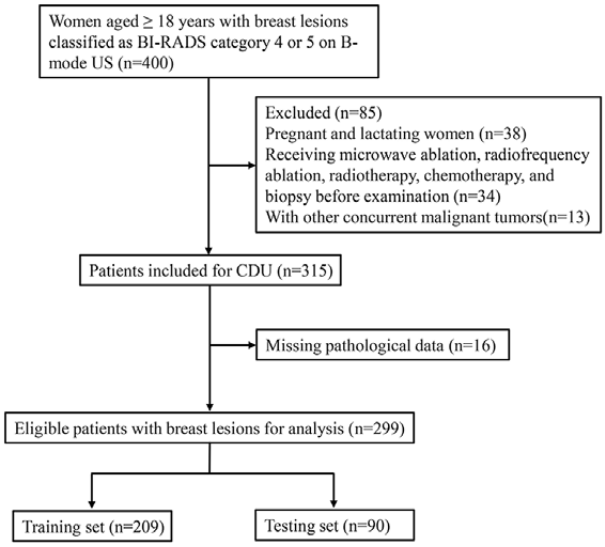

Fig 1. Flowchart of patients' selection.

Results

Participants' selection and characteristics

A total of 400 women with age of ≥18 years old and breast lesions classified as BI-RADS category 4 or 5 were included in this study. Of these, 85 patients were excluded because they were pregnant and lactating women (n=38), received microwave ablation, radiofrequency ablation, radiotherapy, chemotherapy, and biopsy before examination (n=34), and were concurrent with other malignant tumors (n=13). In the remaining 315 patients, 16 of them who were missing pathological data were excluded. Finally, 299 patients were included for analysis, and divided into the training set (n=209) and testing set (n=90) at the ratio of 7: 3 (fig 1). Table I shows that age, BMI, family history, comorbidities, CA15-3, CEA, lesion location, tumor maximum diameter, L/T, BI-RADS category, PI, RI, elasticity score, ADC, and tumor group were comparable between the training and testing sets. In the training set, 84 patients were diagnosed with benign tumors and 125 patients were diagnosed with malignant tumors. We found significant differences in age, BMI, comorbidities, CA15-3, tumor maximum diameter, L/T, BI-RADS category, PI, RI, elasticity score, and ADC between benign group and malignant group (Table II).

Diagnostic performance of single modality

Table III shows the performance of models based on a single modality to diagnose malignant breast lesions. The AUC of the model based on B-mode US, CDU, SE, and MRI was 0.903 (95%CI: 0.857-0.948), 0.940 (95%CI: 0.906-0.974), 0.886 (95%CI: 0.843-0.930), and 0.939 (95%CI: 0.901-0.976), respectively. The internal validation was performed to examine the performance of the model using the testing set. Results displayed that the model based on B-mode US, CDU, SE, and MRI performed well in the diagnosis of malignant lesions, with AUC of 0.884 (95%CI: 0.804-0.964), 0.922 (95%CI: 0.848-0.996), 0.911 (95%CI: 0.847-0.974), and 0.938 (95%CI: 0.888-0.988), respectively, which showed that MRI had the best performance.

Diagnostic performance of combined US modalities

Table IV demonstrates the performance of models based on combined US modalities. The AUC of the model based on B-mode US + CDU, B-mode US + SE, and B-mode US + CDU + SE was 0.976 (95%CI: 0.960-0.993), 0.964 (95%CI: 0.940-0.989), and 0.981 (95%CI: 0.966-0.995), respectively. Further, the performance of models was examined using the testing set. Results of internal validation showed that the model based on B-mode US + CDU, B-mode US + SE, and B-mode US + CDU + SE had a good performance to diagnose malignant lesions. AUC was 0.948 (95%CI: 0.877-1.000), 0.917 (95%CI: 0.844-0.990), and 0.921 (95%CI: 0.845-0.998), respectively, indicating that B-mode US + CDU showed the best performance.

Comparison of performance of MRI and B-mode US + CDU

After adding age, BMI, and CA15-3 to the model, we found B-mode US + CDU and MRI remained the best performance, with AUC of 0.974 (95%CI: 0.955-0.993) and 0.962 (95%CI: 0.939-0.985) in the training set and 0.942 (95%CI: 0.886-0.998) and 0.937 (95%CI: 0.889-0.985) in the testing set (Table V). A DeLong test was performed to compare the AUC from B-mode US + CDU alone with MRI alone or both additionally adding age, BMI, and CA15-3. Results showed that there was not

a significant difference in the performance between B-mode US + CDU and MRI (p=0.786). Adding age, BMI, and CA15-3 did not improve the capacity of the model based on B-mode US + CDU (p= p0.788) and MRI (p=0.804) (Table VI).

Discussion

Our study explored the diagnostic value of US modalities and MRI in malignant breast lesions. Results showed the best performance of MRI and B-mode US + CDU in the diagnosis of malignant breast lesions. There was no significant difference in the performance between B-mode US + CDU and MRI to diagnose malignant breast lesions. The performance was not improved with the addition of demographic data and tumor markers.

MRI has been proven to be an advanced diagnostic tool and has good sensitivity and specificity [5,6]. In this study, we found the best performance of MRI to diagnose malignant breast lesions. Despite the potential benefits, there are barriers to a wider use of MRI, primarily owing to the limited availability and cost-effectiveness. First, it

Table I. Comparison of characteristics between training set and testing set

Variables	Total (n=299)	Training set (n=209)	Testing set (n=90)	Statistics	P
Age, Mean ± SD	49.78 ± 12.08	49.45 ± 12.12	50.56 ± 12.02	t = -0.73	0.467
BMI, Mean ± SD	22.58 ± 1.98	22.65 ± 2.10	22.43 ± 1.65	t = 0.94	0.346
Family history, n (%)				χ^2 = 0.000	0.988
No	246 (82.27)	172 (82.30)	74 (82.22)		
Yes	53 (17.73)	37 (17.70)	16 (17.78)		
Comorbidities, n (%)				χ^2 = 3.209	0.073
No	268 (89.63)	183 (87.56)	85 (94.44)		
Yes	31 (10.37)	26 (12.44)	5 (5.56)		
CA15-3, M (Q_1, Q_3)	9.43 (6.96,18.67)	9.23 (6.89,17.15)	10.16 (7.00,20.59)	Z = 1.323	0.186
CEA, M (Q_1, Q_3)	2.01 (1.36,3.21)	2.04 (1.31,3.46)	2.00 (1.45,2.90)	Z = -0.242	0.809
Lesion location, n (%)				χ^2 = 0.013	0.909
Left breast	148 (49.50)	103 (49.28)	45 (50.00)		
Right breast	151 (50.50)	106 (50.72)	45 (50.00)		
Tumor maximum diameter, M (Q_1, Q_3)	19.00 (13.00,27.00)	19.00 (13.00,26.00)	18.00 (12.00,30.00)	Z = -0.004	0.997
L/T, n (%)				χ^2 = 0.699	0.403
< 1	190 (63.55)	136 (65.07)	54 (60.00)		
≥ 1	109 (36.45)	73 (34.93)	36 (40.00)		
BI-RADS category, n (%)				χ^2 = 1.013	0.798
4a	134 (44.82)	96 (45.93)	38 (42.22)		
4b	47 (15.72)	31 (14.83)	16 (17.78)		
4c	60 (20.07)	40 (19.14)	20 (22.22)		
5	58 (19.40)	42 (20.10)	16 (17.78)		
PI, Mean ± SD	1.30 ± 0.29	1.29 ± 0.30	1.31 ± 0.27	t = -0.54	0.590
RI, Mean ± SD	0.70 ± 0.10	0.70 ± 0.11	0.70 ± 0.09	t = -0.27	0.788
Elasticity score, n (%)				χ^2 = 0.103	0.950
3	101 (33.78)	70 (33.49)	31 (34.44)		
4	183 (61.20)	128 (61.24)	55 (61.11)		
5	15 (5.02)	11 (5.26)	4 (4.44)		
ADC, M (Q_1, Q_3)	0.86 (0.72,1.20)	0.86 (0.73,1.20)	0.88 (0.70,1.18)	Z = -0.953	0.340
Tumor group, n (%)				χ^2 = 1.699	0.192
Benign	113 (37.79)	84 (40.19)	29 (32.22)		
Malignant	186 (62.21)	125 (59.81)	61 (67.78)		

BMI, body mass index; CA15-3, carbohydrate antigen 15-3; CEA, carcinoembryonic antigen; L/T, longitudinal/transverse diameter; BI-RADS, Breast Imaging Reporting and Data System; PI, pulsatility index; RI, resistance index; ADC, apparent diffusion coefficient.

is considered a minimally invasive procedure because of the necessary application of intravenous contrast medium [6]. Second, on average, typical acquisition requires 20 to 30 minutes per examination [6]. For patients, it is less well tolerated for the need of intravenous contrast and longer examination duration. Moreover, the current cost of MRI examination may be prohibitive. Although MRI diagnosis is cost-effective in very high-risk women, it is less likely to be cost-effective in moderate-risk or average-risk women [12,13].

US is a complementary modality for further assessment of suspected mammographic lesions and has been reported as a choice to evaluate dense breasts [14]. It is relatively cheap, safe, and easy to apply without imposing additional contrast medium or radiation [7]. US has shown good results in differentiating malignant lesions from benign ones [15]. Morphologic imaging with B-mode US as a single parameter is a widely used technique for characterizing breast lesions. An important disadvantage of B-mode is the low specificity, resulting in a large number of false-positive results, which have caused unnecessary and false-positive biopsy recommendations [16,17]. In addition to B-mode, several functional US-based modalities were developed to improve the diagnostic performance of breast US [18]. Three combinations of US modalities were evaluated in our study, with B-mode US + CDU showing the best diagnostic performance. Numerous studies have reported the usefulness of CDU

Table II. Characteristics of training set

Variables	Total (n=209)	Benign (n=84)	Malignant (n=125)	Statistics	p
Age, Mean ± SD	49.45 ± 12.12	41.70 ± 8.79	54.65 ± 11.25	t = -9.32	< 0.001
BMI, Mean ± SD	22.65 ± 2.10	21.84 ± 1.57	23.19 ± 2.24	t = -5.15	< 0.001
Family history, n (%)				χ^2 = 3.241	0.072
No	172 (82.30)	74 (88.10)	98 (78.40)		
Yes	37 (17.70)	10 (11.90)	27 (21.60)		
Comorbidities, n (%)				χ^2 = 10.142	0.001
No	183 (87.56)	81 (96.43)	102 (81.60)		
Yes	26 (12.44)	3 (3.57)	23 (18.40)		
CA15-3, M (Q_1, Q_3)	9.23 (6.89,17.15)	8.20 (5.80,10.93)	10.69 (7.40,18.95)	Z = -3.231	0.001
CEA, M (Q_1, Q_3)	2.04 (1.31,3.46)	1.90 (1.39,2.92)	2.21 (1.27,3.76)	Z = -0.934	0.350
Lesion location, n (%)				χ^2 = 0.013	0.911
Left breast	103 (49.28)	41 (48.81)	62 (49.60)		
Right breast	106 (50.72)	43 (51.19)	63 (50.40)		
Tumor maximum diameter, M (Q_1, Q_3)	19.00 (13.00,26.00)	15.00 (10.00,21.00)	22.00 (16.00,29.00)	Z = -5.469	< 0.001
L/T, n (%)				χ^2 = 60.759	< 0.001
< 1	136 (65.07)	81 (96.43)	55 (44.00)		
≥ 1	73 (34.93)	3 (3.57)	70 (56.00)		
BI-RADS category, n (%)				χ^2 = 131.625	< 0.001
4a	96 (45.93)	79 (94.05)	17 (13.60)		
4b	31 (14.83)	3 (3.57)	28 (22.40)		
4c	40 (19.14)	2 (2.38)	38 (30.40)		
5	42 (20.10)	0 (0.00)	42 (33.60)		
PI, Mean ± SD	1.29 ± 0.30	1.07 ± 0.16	1.44 ± 0.28	t = -12.17	< 0.001
RI, Mean ± SD	0.70 ± 0.11	0.63 ± 0.11	0.74 ± 0.07	t = -8.54	< 0.001
Elasticity score, n (%)				χ^2 = 128.959	< 0.001
3	70 (33.49)	66 (78.57)	4 (3.20)		
4	128 (61.24)	18 (21.43)	110 (88.00)		
5	11 (5.26)	0 (0.00)	11 (8.80)		
ADC, M (Q_1, Q_3)	0.86 (0.73,1.20)	1.27 (1.12,1.36)	0.76 (0.67,0.85)	Z = 10.748	< 0.001

BMI, body mass index; CA15-3, carbohydrate antigen 15-3; CEA, carcinoembryonic antigen; L/T, longitudinal/transverse diameter; BI-RADS, Breast Imaging Reporting and Data System; PI, pulsatility index; RI, resistance index; ADC, apparent diffusion coefficient.

Table III. Diagnostic performance of single modality

Model	Set	AUC (95%CI)	Sensitivity (95%CI)	Specificity (95%CI)	PPV (95%CI)	NPV (95%CI)	Accuracy (95%CI)
B-mode US	Training set	0.903(0.857-0.948)	0.856(0.794-0.918)	0.964(0.925-1.004)	0.973(0.942-1.003)	0.818(0.742-0.894)	0.900(0.859-0.940)
	Testing set	0.884(0.804-0.964)	0.721(0.609-0.834)	0.966(0.899-1.032)	0.978(0.935-1.021)	0.622(0.481-0.764)	0.800(0.717-0.883)
CDU	Training set	0.940(0.906-0.974)	0.920(0.872-0.968)	0.929(0.873-0.984)	0.950(0.912-0.989)	0.886(0.820-0.953)	0.923(0.887-0.959)
	Testing set	0.922(0.848-0.996)	0.885(0.805-0.965)	0.931(0.839-1.023)	0.964(0.916-1.013)	0.794(0.658-0.930)	0.900(0.838-0.962)
SE	Training set	0.886(0.843-0.930)	0.968(0.937-0.999)	0.786(0.698-0.873)	0.871(0.815-0.926)	0.943(0.888-0.997)	0.895(0.853-0.936)
	Testing set	0.911(0.847-0.974)	0.918(0.849-0.987)	0.897(0.786-1.007)	0.949(0.893-1.005)	0.839(0.709-0.968)	0.911(0.852-0.970
MRI	Training set	0.939(0.901-0.976)	0.944(0.904-0.984)	0.917(0.858-0.976)	0.944(0.904-0.984)	0.917(0.858-0.976)	0.933(0.899-0.967
	Testing set	0.938(0.888-0.988)	0.869(0.784-0.954)	0.828(0.690-0.965)	0.914(0.842-0.986)	0.750(0.600-0.900)	0.856(0.783-0.928)

AUC, area under the curve; CI, confidence intervals; PPV, positive predictive value; NPV, negative predictive value; US, ultrasound; CDU, color Doppler ultrasounds; SE, strain elastography; MRI, magnetic resonance imaging.

Table IV. Diagnostic performance of combined US modalities

Model	Set	AUC (95%CI)	Sensitivity (95%CI)	Specificity (95%CI)	PPV (95%CI)	NPV (95%CI)	Accuracy(95%CI)
B-mode US + CDU	Training set	0.976(0.960-0.993)	0.968(0.937-0.999)	0.905(0.842-0.968)	0.938(0.896-0.980)	0.950(0.902-0.998)	0.943(0.911-0.974)
	Testing set	0.948(0.877-1.000)	0.902(0.827-0.976)	0.931(0.839-1.023)	0.965(0.917-1.013)	0.818(0.687-0.950)	0.911(0.852-0.970
B-mode US + SE	Training set	0.964(0.940-0.989)	0.904(0.852-0.956)	0.940(0.890-0.991)	0.958(0.921-0.994)	0.868(0.799-0.938)	0.919(0.882-0.956)
	Testing set	0.917(0.844-0.990)	0.885(0.805-0.965)	0.966(0.899-1.032)	0.982(0.947-1.017)	0.800(0.667-0.933)	0.911(0.852-0.970
B-mode US + CDU + SE	Training set	0.981(0.966-0.995)	0.928(0.883-0.973)	0.952(0.907-0.998)	0.967(0.935-0.999)	0.899(0.836-0.962)	0.938(0.905-0.971)
	Testing set	0.921(0.845-0.998)	0.885(0.805-0.965)	0.966(0.899-1.032)	0.982(0.947-1.017)	0.800(0.667-0.933)	0.911(0.852-0.970)

AUC, area under the curve; CI, confidence intervals; PPV, positive predictive value; NPV, negative predictive value; US, ultrasound; CDU, color Doppler ultrasounds; SE, strain elastography.

Table V. Diagnostic performance of MRI and B-mode US + CDU

Model	Set	AUC (95%CI)	Sensitivity (95%CI)	Specificity (95%CI)	PPV (95%CI)	NPV (95%CI)	Accuracy (95%CI)
B-mode US + CDU	Training set	0.976 (0.960-0.993)	0.968 (0.937-0.999)	0.905 (0.842-0.968)	0.938 (0.896-0.980)	0.950 (0.902-0.998)	0.943 (0.911-0.974)
	Testing set	0.948 (0.877-1.000)	0.902 (0.827-0.976)	0.931 (0.839-1.023)	0.965 (0.917-1.013)	0.818 (0.687-0.950)	0.911 (0.852-0.970
MRI	Training set	0.939 (0.901-0.976)	0.944 (0.904-0.984)	0.917 (0.858-0.976)	0.944 (0.904-0.984)	0.917 (0.858-0.976)	0.933 (0.899-0.967
	Testing set	0.938 (0.888-0.988)	0.869 (0.784-0.954)	0.828 (0.690-0.965)	0.914 (0.842-0.986)	0.750 (0.600-0.900)	0.856 (0.783-0.928)
B-mode US + CDU*	Training set	0.974 (0.955-0.993)	0.928 (0.883-0.973)	0.940 (0.890-0.991)	0.959 (0.923-0.994)	0.898 (0.834-0.961)	0.933 (0.899-0.967)
	Testing set	0.942 (0.886-0.998)	0.902 (0.827-0.976)	0.931 (0.839-1.000)	0.965 (0.917-1.000)	0.965 (0.917-1.013)	0.911 (0.852-0.970)
MRI*	Training set	0.962 (0.939-0.985)	0.896 (0.842-0.950)	0.929 (0.873-0.984)	0.949 (0.910-0.989)	0.857 (0.785-0.929)	0.909 (0.870-0.948)
	Testing set	0.937 (0.889-0.985)	0.820 (0.723-0.916)	0.897 (0.786-1.007)	0.943 (0.881-1.006)	0.703 (0.555-0.850)	0.844 (0.770-0.919)

AUC, area under the curve; CI, confidence intervals; PPV, positive predictive value; NPV, negative predictive value; US, ultrasound; CDU, color Doppler ultrasounds; MRI, magnetic resonance imaging.
* indicated that this model additionally included age, BMI, and CA15-3.

Table VI. Comparison of diagnostic performance of MRI and B-mode US + CDU

Model	AUC (95%CI)	Statistics	p
B-mode US + CDU	0.948 (0.877-1.000)	Ref	
MRI	0.938 (0.888-0.988)	0.271	0.786
B-mode US + CDU*	0.942 (0.886-0.998)	0.269	0.788
MRI*	0.937 (0.889-0.985)	0.248	0.804

AUC, area under the curve; CI, confidence intervals; US, ultrasound; CDU, color Doppler ultrasounds; MRI, magnetic resonance imaging.
* indicated that this model additionally included age, BMI, and CA15-3.

in breast lesions [19]. The Japan Association of Breast and Thyroid Sonology (JABTS) performed a large-scale study, and its results revealed that vessels, vascular flow patterns, and incident angle were useful for differential diagnosis of benign and malignant disease [19]. The simulation experiments of Watanabe et al revealed that combination of B-mode and CDU significantly improved the specificity of B-mode alone [20]. Qian et al reported the good diagnostic performance of B-mode and CDU used in combination [21]. In this study, we also found that the performance of the combination of B-mode and CDU outperformed B-mode alone.

In this study, we also showed there was no significant difference in the diagnostic performance between MRI and combination of B-mode and CDU, indicating that B-mode combined with CDU could be as an alternative if MRI could not be performed. It is obvious that combination of B-mode and CDU provided a relatively low-cost based on providing both morphological and functional information although formal cost-effectiveness analysis was not performed. Le-Petross et al agreed that MRI was limited by its cost and availability, and it is not recommended for women with low to moderate risk of developing breast cancer [22]. The diagnostic performance of B-mode + CDU was comparable to MRI, with slightly higher sensitivity and specificity than MRI; in addition, B-mode + CDU was likely to demonstrate lower costs and better accessibility. Studies have illustrated the importance of demographic data and tumor markers in the diagnosis of breast lesions [23,24]. Our study found the addition of demographic data and tumor markers did not improve the performance of B-mode and CDU used in combination, which suggested the robustness of our model.

This study has some advantages. First, this study compares the performance of single or combined US with MRI in the diagnosis of malignant breast lesions and determines B-mode + CDU as a non-invasive, safe, and economic modality for high-risk patients, providing a reference for the rational allocation of medical resources. Second, only patients those who have been diagnosed by pathology were included in this study, and this makes models more accurate.

However, some limitations exist in this study. First, patients included in this study are those who classified as BI-RADS category 4 or 5, which limits our findings popularized in general population. Second, this is a single-center study, and the inclusion criteria are strict, which may prove some selection bias. Multi-center studies are required to verify our findings in the future. Third, CDU and SE are performed after B-mode US, and B-mode US results may affect the judgment on subsequent inspections.

Conclusion

Our study found that the diagnostic performance between B-mode + CDU and MRI was comparable, indicating that B-mode + CDU might be an alternative to MRI. In the clinical settings, clinicians should give priority to the combination of B-mode and CDU for the purpose of time-saving and economic considerations and providing guidance for the decision on biopsy to decrease biopsy recommendations.

Conflict of interest: none

References

1. Fahad Ullah M. Breast Cancer: Current Perspectives on the Disease Status. Adv Exp Med Biol 2019;1152:51-64.
2. Pfeiffer RM, Webb-Vargas Y, Wheeler W, Gail MH. Proportion of U.S. Trends in Breast Cancer Incidence Attributable to Long-term Changes in Risk Factor Distributions. Cancer Epidemiol Biomarkers Prev 2018;27:1214-1222.
3. Siegel RL, Miller KD, Fuchs HE, Jemal A. Cancer statistics, 2022. CA Cancer J Clin 2022;72:7-33.
4. Tan PH, Ellis I, Allison K, et al. The 2019 World Health Organization classification of tumours of the breast. Histopathology 2020;77:181-185.
5. Vreemann S, Gubern-Mérida A, Schlooz-Vries MS, et al. Influence of Risk Category and Screening Round on the Performance of an MR Imaging and Mammography Screening Program in Carriers of the BRCA Mutation and Other Women at Increased Risk. Radiology 2018;286:443-451.
6. Gao Y, Reig B, Heacock L, Bennett DL, Heller SL, Moy L. Magnetic Resonance Imaging in Screening of Breast Cancer. Radiol Clin North Am 2021;59:85-98.
7. Guo R, Lu G, Qin B, Fei B. Ultrasound Imaging Technologies for Breast Cancer Detection and Management: A Review. Ultrasound Med Biol 2018;44:37-70.
8. Ranjkesh M, Hajibonabi F, Seifar F, Tarzamni MK, Moradi B, Khamnian Z. Diagnostic Value of Elastography,

Strain Ratio, and Elasticity to B-Mode Ratio and Color Doppler Ultrasonography in Breast Lesions. Int J Gen Med 2020;13:215-224.
9. Li L, Zhou X, Zhao X, et al. B-Mode Ultrasound Combined with Color Doppler and Strain Elastography in the Diagnosis of Non-mass Breast Lesions: A Prospective Study. Ultrasound Med Biol 2017;43:2582-2590.
10. Shiina T, Nightingale KR, Palmeri ML, et al. WFUMB guidelines and recommendations for clinical use of ultrasound elastography: Part 1: basic principles and terminology. Ultrasound Med Biol. 2015;41:1126-1147.
11. Iversen DS, Kesmodel US, Ovesen PG. Associations between parity and maternal BMI in a population-based cohort study. Acta Obstet Gynecol Scand 2018;97:694-700.
12. Taneja C, Edelsberg J, Weycker D, Guo A, Oster G, Weinreb J. Cost effectiveness of breast cancer screening with contrast-enhanced MRI in high-risk women. J Am Coll Radiol. 2009;6:171-179.
13. Pataky R, Armstrong L, Chia S, et al. Cost-effectiveness of MRI for breast cancer screening in BRCA1/2 mutation carriers. BMC Cancer 2013;13:339.
14. Kim SH, Kim HH, Moon WK. Automated Breast Ultrasound Screening for Dense Breasts. Korean J Radiol 2020;21:15-24.
15. Meel-van den Abeelen AS, Weijers G, van Zelst JC, Thijssen JM, Mann RM, de Korte CL. 3D quantitative breast ultrasound analysis for differentiating fibroadenomas and carcinomas smaller than 1cm. Eur J Radiol 2017;88:141-147.
16. Cho N, Jang M, Lyou CY, Park JS, Choi HY, Moon WK. Distinguishing benign from malignant masses at breast US: combined US elastography and color doppler US-influence on radiologist accuracy. Radiology 2012;262: 80-90.
17. Berg WA, Zhang Z, Lehrer D, et al. Detection of breast cancer with addition of annual screening ultrasound or a single screening MRI to mammography in women with elevated breast cancer risk. JAMA 2012;307:1394-1404.
18. Kapetas P, Clauser P, Woitek R, et al. Quantitative Multiparametric Breast Ultrasound: Application of Contrast-Enhanced Ultrasound and Elastography Leads to an Improved Differentiation of Benign and Malignant Lesions. Invest Radiol 2019;54:257-264.
19. Watanabe T, Kaoku S, Yamaguchi T, et al. Multicenter Prospective Study of Color Doppler Ultrasound for Breast Masses: Utility of Our Color Doppler Method. Ultrasound Med Biol. 2019;45:1367-1379.
20. Watanabe T, Yamaguchi T, Okuno T, et al. Utility of B-Mode, Color Doppler and Elastography in the Diagnosis of Breast Cancer: Results of the CD-CONFIRM Multicenter Study of 1351 Breast Solid Masses. Ultrasound Med Biol. 2021;47:3111-3121.
21. Qian X, Zhang B, Liu S, et al. A combined ultrasonic B-mode and color Doppler system for the classification of breast masses using neural network. Eur Radiol. 2020;30:3023-3033.
22. Le-Petross HT, Shetty MK. Magnetic resonance imaging and breast ultrasonography as an adjunct to mammographic screening in high-risk patients. Semin Ultrasound CT MR 2011;32:266-272.
23. Saadaat R, Abdul-Ghafar J, Haidary AM, Rahmani S, Atta N. Age distribution and types of breast lesions among Afghan women diagnosed by fine needle aspiration cytology (FNAC) at a tertiary care centre in Afghanistan: a descriptive cross-sectional study. BMJ Open 2020;10:e037513.
24. Bonacho T, Rodrigues F, Liberal J. Immunohistochemistry for diagnosis and prognosis of breast cancer: a review. Biotech Histochem 2020;95:71-91.